

# Numerical Simulations of White Dwarf Tidal Disruption Events

Sinead Humphrey\*

*Department of Physics, University of Wisconsin-Milwaukee  
Milwaukee, WI, United States of America*

## Abstract

Numerical simulations of white dwarf tidal disruption events are performed using the 3-D moving-mesh hydrodynamic code, MANGA. In order to study the effect of nuclear burning on these events, we add a nuclear burning module to MANGA. Here, we present preliminary results from two simulations of white dwarf tidal disruption events with nuclear burning. We see no nuclear burning for shallow penetration; however, we see significant nuclear burning for deep penetration. Significant nuclear burning that produces radioactive elements will likely affect the light curve and observability of these events.

## 1. Introduction

Most main sequence stars will end their life as white dwarfs (WDs) which are the remnant carbon and oxygen cores of red giants and asymptotic giant branch stars. WDs no longer undergo fusion but are instead supported against collapse by electron degeneracy pressure. They are therefore extremely dense; a  $1M_{\odot}$  WD would have a radius similar to that of the Earth.

If a WD passes close enough to a black hole, it can be torn apart by tidal forces in a WD tidal disruption event (WDTDE). In order to be tidally disrupted, the WD must pass within the tidal radius  $r_t$  of the black hole.

$$r_t = R_{\text{WD}}(M_{\text{BH}}/M_{\text{WD}})^{1/3} \quad (1)$$

where  $R_{\text{WD}}$  is the radius of the WD,  $M_{\text{BH}}$  is the mass of the black hole, and  $M_{\text{WD}}$  is the mass of the WD.

Because of how the tidal radius scales with the mass of the black hole, only intermediate mass ( $10^3 - 10^5 M_{\odot}$ ) black holes (IMBHs) are capable of disrupting a WD (Maguire et al. 2020). This is notable as IMBHs have yet to be directly detected. A single observation of a WDTDE would serve as a direct detection of an IMBH; several detections would allow us to probe the population of IMBHs which may give us insight into how black holes evolve in the universe. The WDTDEs also differ from stellar tidal disruption events (TDEs) in that they have the potential to ignite thermonuclear reactions which may give them a unique electromagnetic signal (Maguire et al., 2020).

The strength of a WDTDE is characterized by the impact parameter,  $\beta$  defined as

$$\beta = \frac{r_t}{r_p}, \quad (2)$$

where  $r_p$  is the distance of closest approach. A higher  $\beta$  corresponds to a deeper penetration. Spaulding and Chang (2021) found that, for stellar TDEs, the energy spread of the debris scaled as  $\beta^{1/2}$  for  $\beta$  values from 2 to 9 and asymptotes for  $\beta \gtrsim 10$ . This energy spread may manifest itself as different compression ratios and thus may also affect nuclear burning in WDTDEs. It is also expected that less massive WDs may require deeper penetration into the tidal radius (higher  $\beta$ ) in order to ignite (Rosswog et al. 2009).

---

\*This author is supported by NASA under Award No. RPF22-8-0 through the Wisconsin Space Grant Consortium Graduate and Professional Research Fellowship. We use the YT python package for the analysis of the data and generation of plots in this work (Turk et al., 2011). Computational work was done on the University of Wisconsin-Milwaukee High Performance Computing cluster, Mortimer.

**1.1. Numerical Simulations.** WDTDEs combine the physics of gravity, degeneracy pressure, and nuclear burning in a highly non-linear system making them difficult to study analytically. In order to better understand them we rely on high resolution, realistic 3-D numerical simulations.

There are two dominant methodologies that are used to numerically solve hydrodynamic equations: smoothed particle hydrodynamics (SPH) and Eulerian solvers. SPH does well at maintaining conserved quantities, but due to its smoothing, it is not well suited to discontinuities. Eulerian solvers are much better suited to capturing discontinuities such as shocks, but they do not obey conservation laws well (Springel, 2010). Recently, however, arbitrary Lagrangian-Eulerian (ALE) schemes have been introduced. These ALE or moving-mesh codes combine the superior conservation properties of SPH with the shock capturing of Eulerian schemes and are well suited to solving a number of astrophysical problems including WDTDEs.

## 2. Methodology

We use the moving-mesh hydrodynamic code, MANGA (Chang et al., 2017; Prust and Chang, 2019; Chang et al., 2020; Chang and Etienne, 2020), to simulate WDTDEs. MANGA solves the Euler equations with (self-)gravity, which written in conservative form are:

$$\frac{\partial \rho}{\partial t} + \nabla \cdot \rho \mathbf{v} = 0 \quad (3)$$

$$\frac{\partial \rho \mathbf{v}}{\partial t} + \nabla \cdot \rho \mathbf{v} \mathbf{v} + \nabla P = -\rho \nabla \Phi \quad (4)$$

$$\frac{\partial \rho e}{\partial t} + \nabla \cdot (\rho e + P) \mathbf{v} = -\rho \mathbf{v} \cdot \nabla \Phi \quad (5)$$

where  $\rho$  is density,  $P$  is pressure,  $\mathbf{v}$  is velocity,  $\Phi$  is the gravitational potential, and  $e$  is the specific energy. These equations can be rewritten in a more compact notation by introducing a state vector  $\mathcal{U} = (\rho, \rho \mathbf{v}, \rho e)$ :

$$\frac{\partial \mathcal{U}}{\partial t} + \nabla \cdot \mathcal{F} = \mathcal{S} \quad (6)$$

where  $\mathcal{F} = (\rho \mathbf{v}, \rho \mathbf{v} \mathbf{v}, (\rho e + P) \mathbf{v})$  is the flux function and  $\mathcal{S} = (0, -\rho \nabla \Phi, -\rho \mathbf{v} \cdot \nabla \Phi)$  is the source function (Chang et al. 2017).

**2.1. Inclusion of Nuclear Burning.** In order to introduce nuclear burning, an additional term to the source function for energy was added:

$$-\rho \mathbf{v} \cdot \nabla \Phi \rightarrow -\rho \mathbf{v} \cdot \nabla \Phi + \rho \epsilon_{\text{nuc}}, \quad (7)$$

where  $\epsilon_{\text{nuc}}$  is the nuclear energy generation rate.

Additional equations to track the abundance of different isotopes were also added. We used the nuclear reaction network, approx21 (Timmes et al., 2000), that is implemented in MESA (Paxton et al., 2011, 2013, 2015, 2018; Paxton, 2019). Approx21 includes 21 species: n, p,  $^1\text{H}$ ,  $^3\text{He}$ ,  $^4\text{He}$ ,  $^{12}\text{C}$ ,  $^{14}\text{N}$ ,  $^{16}\text{O}$ ,  $^{20}\text{Ne}$ ,  $^{24}\text{Mg}$ ,  $^{28}\text{Si}$ ,  $^{32}\text{S}$ ,  $^{36}\text{Ar}$ ,  $^{40}\text{Ca}$ ,  $^{44}\text{Ti}$ ,  $^{48}\text{Cr}$ ,  $^{56}\text{Cr}$ ,  $^{52}\text{Fe}$ ,  $^{54}\text{Fe}$ ,  $^{56}\text{Fe}$ ,  $^{56}\text{Ni}$ . This involves adding 21 scalar equations to the solver, which are of the form:

$$\frac{\partial \rho X_i}{\partial t} + \nabla \cdot \rho X_i \mathbf{v} = \mathcal{S}_i(x_1, \dots, x_n), \quad (8)$$

where  $X_i$  are the fractional (by mass) abundance of species  $i$ , and  $\mathcal{S}_i$  is the source function due to nuclear burning for species  $i$ .

## 3. Results

We performed two simulations of WDTDEs in MANGA with the new nuclear burning module at low resolution. We model a 50-50 carbon-oxygen  $0.6M_{\odot}$  WD with 25,000 mesh-generating points and include an atmosphere with density  $\rho = 0.01 \text{ g cm}^{-3}$ . The total number of mesh generating points in each simulation is 54,758 with 25,000 points modeling the WD. We model the IMBH as a softened  $10^4 M_{\odot}$  dark matter particle.

We performed one simulation with  $\beta = 2$  and one with  $\beta = 5$ . Figures 1 and 2 show four frames that are 1.5 seconds apart of the WD being tidally disrupted by the IMBH. Moving from frame 1 in the upper left to frame 4 in the lower right, we see that the WDs are completely disrupted by the end. The simulation with  $\beta = 5$  shows the WD passing closer to the IMBH causing the gas of the WD to spread out further than in the simulation with  $\beta = 2$ .

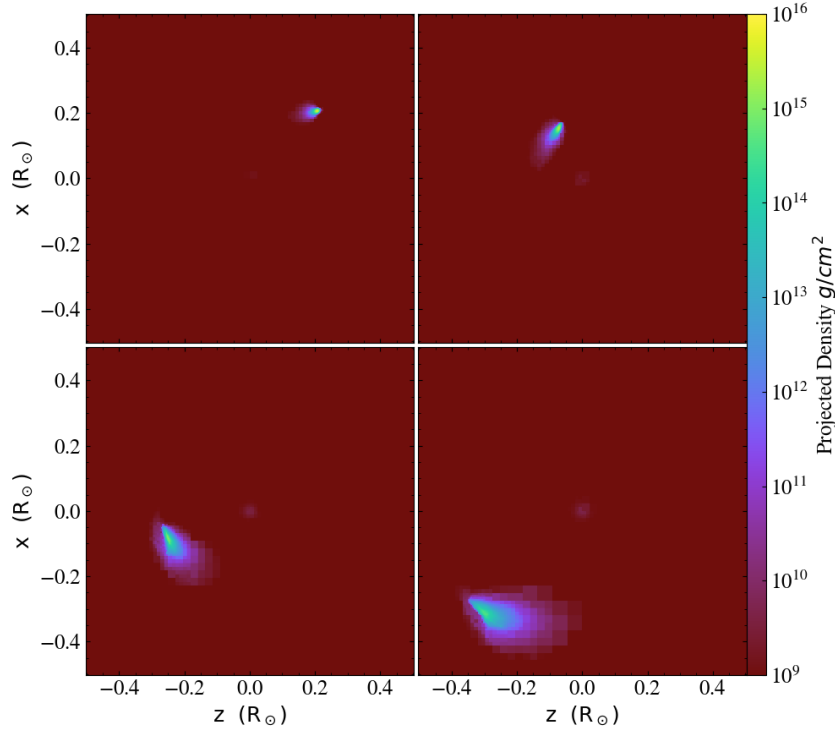


Figure 1: The projected density of a WD undergoing tidal disruption simulated in MANGA with 25,000 mesh-generating points used for the WD. We used a black hole with a mass of  $10^4 M_\odot$ , a WD with a mass of  $0.6 M_\odot$ , and  $\beta = 2$ . Each frame is 1.5 seconds apart.

The simulation with  $\beta = 2$  experienced negligible nuclear burning. However, the simulation with  $\beta = 5$  underwent significant nuclear burning. Figure 3 shows the mass fraction of the isotopes  $^{12}\text{C}$ ,  $^{16}\text{O}$ ,  $^{20}\text{Ne}$ ,  $^{24}\text{Mg}$ ,  $^{28}\text{Si}$ , and  $^{56}\text{Ni}$ . We can see that, initially, the WD is 50%  $^{12}\text{C}$  and 50%  $^{16}\text{O}$ , but as it becomes disrupted it begins to burn much of its  $^{12}\text{C}$  which leads to an initial increase in  $^{16}\text{O}$ ,  $^{20}\text{Ne}$ ,  $^{24}\text{Mg}$ , and  $^{28}\text{Si}$  at around 5.6 seconds. We see at about 6.25 seconds that  $^{16}\text{O}$  also begins to burn shortly before the abundances level off at around 7 seconds.

We calculated the energy created from nuclear burning ( $E_{\text{burn}}$ ) in ergs by using the binding energies of the isotopes and found that  $E_{\text{burn}} = 4 \times 10^{50}$  ergs. We also found that about  $0.3 M_\odot$  of gas burned and  $0.002 M_\odot$  of iron group elements were created.

#### 4. Discussion

In order to see if our results are reasonable we first compare to Rosswog et al. (2009) who performed SPH simulations of WDTDEs. Compared to run 11 in Rosswog et al. (2009), our initial results seem somewhat consistent. Rosswog et al. use a  $0.6 M_\odot$  WD and a  $\beta$  of 5, similar to our simulation, however it is worth noting they use a  $1000 M_\odot$  BH where we have a  $10,000 M_\odot$  BH. In run 11, Rosswog et al. found  $E_{\text{burn}} \approx 2.7 \times 10^{50}$  ergs which is roughly comparable to our  $E_{\text{burn}} \approx 4 \times 10^{50}$  ergs. We can also compare to the gravitational binding energy of a  $0.6 M_\odot$  WD which is  $1.3 \times 10^{50}$  ergs. Because  $E_{\text{burn}}$  is greater than the gravitational binding energy, nuclear burning likely plays a significant role in the end point of WDTDEs. Rosswog et al. also found that for run 11, there was  $3 \times 10^{-4} M_\odot$  of iron group elements created, whereas we found  $2 \times 10^{-3} M_\odot$ .

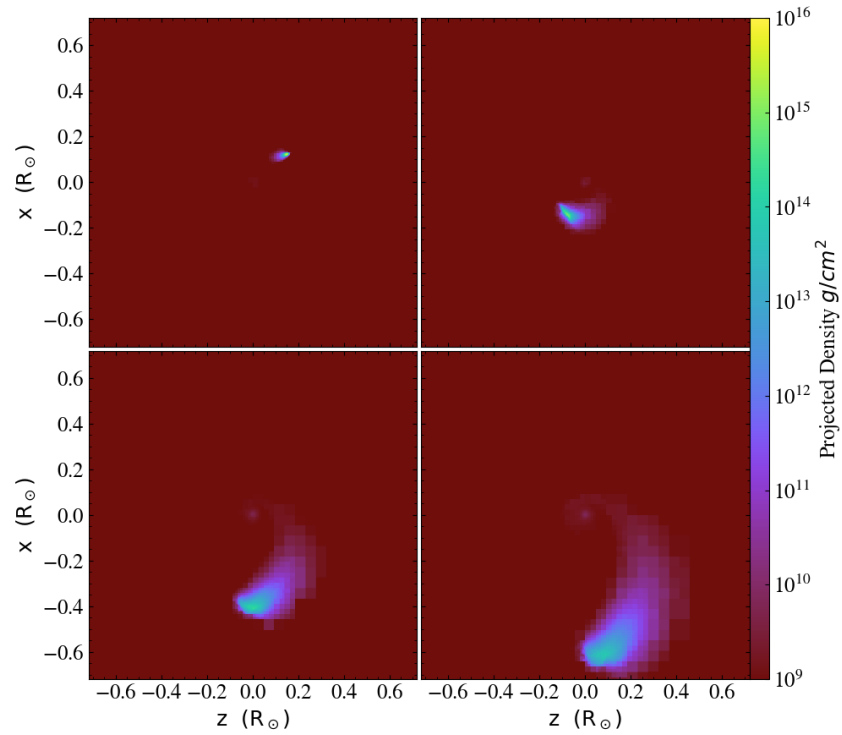


Figure 2: The projected density of a WD undergoing tidal disruption simulated in MANGA with 25,000 mesh-generating points used for the WD. We used a black hole with a mass of  $10^4 M_\odot$ , a WD with a mass of  $0.6 M_\odot$ , and  $\beta = 5$ . Each frame is 1.5 seconds apart.

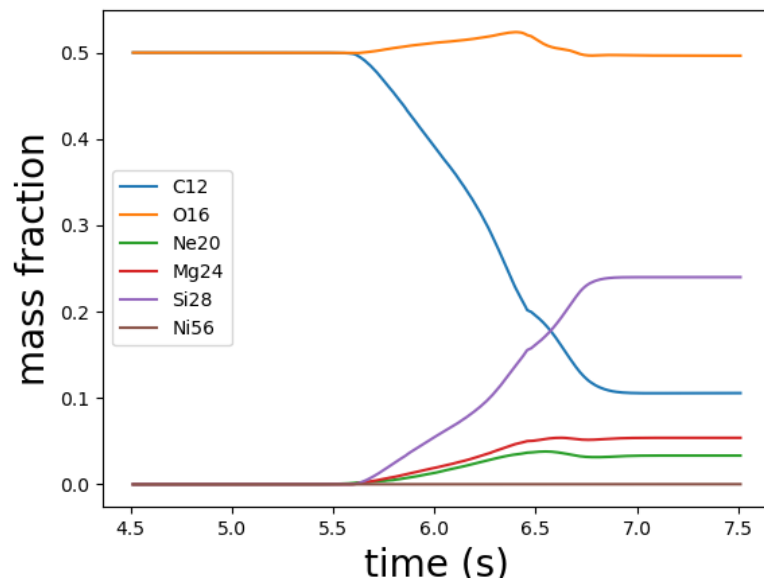


Figure 3: A plot of the mass abundances of various isotopes over time for a simulation of a 50-50 Carbon-Oxygen WD tidally disrupted by a  $10^4 M_\odot$  BH with  $\beta = 5$ .

There are multiple ways in which a WDTDE may be detected; the first being in the rapid accretion onto the BH after disruption, and the second being through radioactive nickel decay. Accretion would be mainly in the x-rays, which might be found by x-ray telescopes like the Neil Gehrels Swift Observatory. However, the Eddington luminosity of IMBHs is rather small ( $\sim 10^{42}$  ergs  $s^{-1}$ ) and so it is likely not detectable at large distances. This is moderated by the fact that such rapid accretion can produce a jet, which would make the apparent luminosity much larger.

Radioactive nickel decay would likely result in significant optical emission, which could be found by large transient surveys such as the Vera Rubin Observatory. A larger parameter study at higher resolution would elucidate the parameter space for which these WDTDEs can be observed. Moreover, the detection or non-detection of these WDTDEs would serve as a major constraint on the population of IMBHs.

## Acknowledgments

We thank Philip Chang for helpful discussion and advice. This work was supported by NASA under Award No. RPF22.8-0 through the Wisconsin Space Grant Consortium Graduate and Professional Research Fellowship. We use the YT python package for the analysis of the data and generation of plots in this work (Turk et al., 2011). Computational work was done on the University of Wisconsin-Milwaukee High Performance Computing cluster, Mortimer.

## References

- P. Chang and Z. B. Etienne. General relativistic hydrodynamics on a moving-mesh i: static space-times. *MNRAS*, 496(1):206–214, jun 2020. doi: 10.1093/mnras/staa1532.
- P. Chang, J. Wadsley, and T. R. Quinn. A moving-mesh hydrodynamic solver for ChaNGa. *MNRAS*, 471:3577–3589, Nov. 2017. doi: 10.1093/mnras/stx1809.
- P. Chang, S. W. Davis, and Y.-F. Jiang. Time-dependent radiation hydrodynamics on a moving mesh. *MNRAS*, 493(4):5397–5407, Apr. 2020. doi: 10.1093/mnras/staa573.
- K. Maguire, M. Eracleous, P. G. Jonker, M. MacLeod, and S. Rosswog. Tidal Disruptions of White Dwarfs: Theoretical Models and Observational Prospects. *SSR*, 216(3):39, Mar. 2020. doi: 10.1007/s11214-020-00661-2.
- B. Paxton. Modules for Experiments in Stellar Astrophysics (MESA). Zenodo, Sept. 2019.
- B. Paxton, L. Bildsten, A. Dotter, F. Herwig, P. Lesaffre, and F. Timmes. Modules for Experiments in Stellar Astrophysics (MESA). *ApJS*, 192:3, Jan. 2011. doi: 10.1088/0067-0049/192/1/3.
- B. Paxton, M. Cantiello, P. Arras, L. Bildsten, E. F. Brown, A. Dotter, C. Mankovich, M. H. Montgomery, D. Stello, F. X. Timmes, and R. Townsend. Modules for Experiments in Stellar Astrophysics (MESA): Planets, Oscillations, Rotation, and Massive Stars. *ApJS*, 208:4, Sept. 2013. doi: 10.1088/0067-0049/208/1/4.
- B. Paxton, P. Marchant, J. Schwab, E. B. Bauer, L. Bildsten, M. Cantiello, L. Dessart, R. Farmer, H. Hu, N. Langer, R. H. D. Townsend, D. M. Townsley, and F. X. Timmes. Modules for Experiments in Stellar Astrophysics (MESA): Binaries, Pulsations, and Explosions. *ApJS*, 220:15, Sept. 2015. doi: 10.1088/0067-0049/220/1/15.
- B. Paxton, J. Schwab, E. B. Bauer, L. Bildsten, S. Blinnikov, P. Duffell, R. Farmer, J. A. Goldberg, P. Marchant, E. Sorokina, A. Thoul, R. H. D. Townsend, and F. X. Timmes. Modules for Experiments in Stellar Astrophysics (MESA): Convective Boundaries, Element Diffusion, and Massive Star Explosions. *ApJS*, 234(2):34, Feb. 2018. doi: 10.3847/1538-4365/aaa5a8.
- L. J. Prust and P. Chang. Common envelope evolution on a moving mesh. *MNRAS*, 486(4):5809–5818, July 2019. doi: 10.1093/mnras/stz1219.
- S. Rosswog, E. Ramirez-Ruiz, and W. R. Hix. Tidal Disruption and Ignition of White Dwarfs by Moderately Massive Black Holes. *ApJ*, 695(1):404–419, Apr. 2009. doi: 10.1088/0004-637X/695/1/404.
- V. Springel. E pur si muove: Galilean-invariant cosmological hydrodynamical simulations on a moving mesh. *MNRAS*, 401:791–851, Jan. 2010. doi: 10.1111/j.1365-2966.2009.15715.x.

F. X. Timmes, R. D. Hoffman, and S. E. Woosley. An Inexpensive Nuclear Energy Generation Network for Stellar Hydrodynamics. *ApJS*, 129(1):377–398, July 2000. doi: 10.1086/313407.

M. J. Turk, B. D. Smith, J. S. Oishi, S. Skory, S. W. Skillman, T. Abel, and M. L. Norman. yt: A Multi-code Analysis Toolkit for Astrophysical Simulation Data. *ApJS*, 192(1):9, Jan. 2011. doi: 10.1088/0067-0049/192/1/9.